POLITECNICO DI TORINO
Repository ISTITUZIONALE

A short review of unconventional riblet designs for skin-friction drag reduction in turbulent flows

Original
A short review of unconventional riblet designs for skin-friction drag reduction in turbulent flows / Amico, E., Cafiero, G.. - In: CHINESE JOURNAL OF AERONAUTICS. - ISSN 1000-9361. - 39:10(2026). [10.1016/j.cja.2026.104278]

Availability:
This version is available at: 11583/3012000 since: 2026-06-13T08:28:54Z

Publisher:
Elsevier

Published
DOI:10.1016/j.cja.2026.104278

Terms of use:

This article is made available under terms and conditions as specified in the corresponding bibliographic description in the repository

Publisher copyright

(Article begins on next page)

19 November 2026

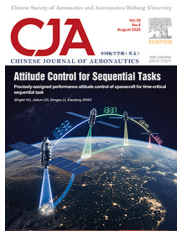
Chinese Journal of Aeronautics, (2026), 39(10): 104278



Chinese Society of Aeronautics and Astronautics
& Beihang University

Chinese Journal of Aeronautics

cja@buaa.edu.cn
www.sciencedirect.com



REVIEW ARTICLE

A short review of unconventional riblet designs for skin-friction drag reduction in turbulent flows



Enrico AMICO, Gioacchino CAFIERO *

Department of Mechanical and Aerospace Engineering, Politecnico di Torino, Corso Duca degli Abruzzi 24, Torino 10129, Italy

Received 13 January 2026; revised 2 February 2026; accepted 1 April 2026
Available online 4 June 2026

KEYWORDS

Innovative surfaces;
Passive drag reduction;
Riblets;
Skin-friction drag;
Turbulent flow

Abstract This paper provides a concise review of riblet-based strategies for skin-friction drag reduction, with a particular focus on emerging and unconventional designs. We first summarize the performance of conventional straight riblets, aligned with the mean flow direction, which are known to achieve drag reductions of up to about 10% under optimal conditions. We then explore alternative riblet geometries that have been proposed to address key limitations of straight configurations, notably their sensitivity to the design point and the rapid degradation of performance under off-design conditions. Concepts such as wavy, converging–diverging, and herringbone riblets suggest new pathways for broadening the operational envelope and potentially achieving enhanced drag-reduction levels. In this context, the integration of advanced optimization frameworks and machine-learning techniques offers a promising avenue for systematically exploring high-dimensional design spaces and uncovering novel riblet configurations with improved robustness and performance.

© 2026 The Author(s). Published by Elsevier Ltd on behalf of Chinese Society of Aeronautics and Astronautics. This is an open access article under the CC BY-NC-ND license (http://creativecommons.org/licenses/by-nc-nd/4.0/).

1. Introduction

In many technologically relevant turbulent flows, skin-friction drag constitutes a dominant contribution to the total drag, particularly for configurations characterised by large wetted surface areas and predominantly attached boundary layers. Typical examples include aircraft wings and fuselages, marine vehicles, turbomachinery components, and internal flow systems such as pipelines and ducts. Because skin friction arises directly from momentum transfer between the wall and the near-wall turbulent structures, even modest reductions can translate into significant performance gains at the system level. Consequently, the reduction of turbulent skin-friction drag has remained a central objective in fluid mechanics and flow-control research for several decades.

The importance of skin-friction drag reduction is especially pronounced in the aeronautical sector. For modern transport aircraft operating in cruise conditions, a substantial fraction of the total aerodynamic drag—often exceeding 40–50%—is associated with viscous effects in turbulent boundary layers over wings, fuselage, nacelles, and control surfaces (see

* Corresponding author.
E-mail address: gioacchino.cafiero@polito.it (G. CAFIERO).

☆ This article is part of a special issue entitled: 'Next-Gen Aerospace Complex Surfaces' published in Chinese Journal of Aeronautics.



Production and hosting by Elsevier

https://doi.org/10.1016/j.cja.2026.104278
1000-9361 © 2026 The Author(s). Published by Elsevier Ltd on behalf of Chinese Society of Aeronautics and Astronautics.
This is an open access article under the CC BY-NC-ND license (http://creativecommons.org/licenses/by-nc-nd/4.0/).

Fig. 1). As emphasised by Kornilov,[1] improvements in skin-friction drag directly impact fuel consumption, operating costs, and environmental footprint. Given the scale of commercial aviation, reductions of only a few percent in total drag can lead to large absolute savings in fuel burn and corresponding reductions in CO_2 emissions over an aircraft's operational lifetime.

From an industrial perspective, skin-friction drag reduction is particularly attractive because it targets losses that scale with surface area rather than with lift or propulsion requirements. In contrast to measures that rely on radical changes to vehicle architecture or operating conditions, surface-based drag-reduction strategies can, in principle, be retrofitted or incrementally integrated into existing designs. This feature is highlighted by Kornilov,[1] who notes that passive drag-reduction technologies—such as riblets, compliant coatings, or surface texturing—are appealing precisely because they offer performance benefits without requiring continuous energy input or active control systems.

In aeronautical applications, the relevance of skin-friction drag reduction extends beyond cruise efficiency alone. Reduced wall shear stress can lead to lower thermal loads, delayed surface degradation, and potentially reduced acoustic emissions associated with boundary-layer turbulence. Moreover, improvements in viscous efficiency can provide additional design freedom, for instance by enabling higher lift-to-drag ratios or extended operational envelopes. These secondary benefits further strengthen the case for sustained research into drag-reduction concepts that are robust, scalable, and compatible with realistic operating environments.

At the same time, the stringent constraints of the aeronautic sector impose demanding requirements on drag-reduction technologies. Any proposed solution must demonstrate not only measurable drag reduction under controlled laboratory conditions, but also robustness to surface contamination, manufacturing tolerances, wear, and off-design flow conditions such as pressure gradients and yaw. As discussed by Kornilov,[1] these practical considerations explain why many drag-reduction concepts that are successful in canonical flows fail to translate directly to industrial deployment, and why long-term validation at relevant Reynolds numbers remains essential.

Within this broader context, riblets occupy a unique position among skin-friction drag-reduction strategies. They are one of the few concepts that have demonstrated consistent drag reduction in laboratory experiments, numerical simulations, and full-scale aeronautical tests. Their relevance to the aeronautic sector lies not only in their demonstrated performance, but also in the fundamental insights they provide into near-wall turbulence manipulation. As such, riblets serve both as a practical drag-reduction technology and as a benchmark for evaluating and developing new approaches aimed at reducing turbulent skin friction in real-world applications.

Overall, the continuing emphasis on fuel efficiency, emissions reduction, and sustainable aviation ensures that skin-friction drag reduction will remain a topic of high relevance. Reviews such as the present one contribute to this effort by consolidating decades of experimental, numerical, and theoretical work, and by clarifying the physical mechanisms and limitations that govern the performance of surface-based drag-reduction strategies in turbulent flows.

Passive devices for skin friction drag reduction have represented one of the key drivers in turbulence control over the past decades. Even more so, with the increasing demand for reduced emissions in the aerospace transportation sector, there is an urge to find solutions that can move from the lab to real life. While aerospace has always represented a key driver for scientific discovery and more specifically for cutting-edge technologies, the use of passive devices for drag reduction is also often found in the automotive, naval, and in the sports aerodynamics sectors.

This review is guided by the following questions: (A) which physical mechanisms are introduced by unconventional layouts; (B) how these mechanisms affect the balance between skin-friction reduction and additional drag penalties; and (C) whether any of these concepts demonstrate robustness and scalability toward realistic flow conditions.

2. Canonical riblets: Mechanism and limitations

Riblets—streamwise-aligned, micro-scale surface grooves—are among the most extensively studied passive strategies for turbulent skin-friction drag reduction. Their effectiveness has

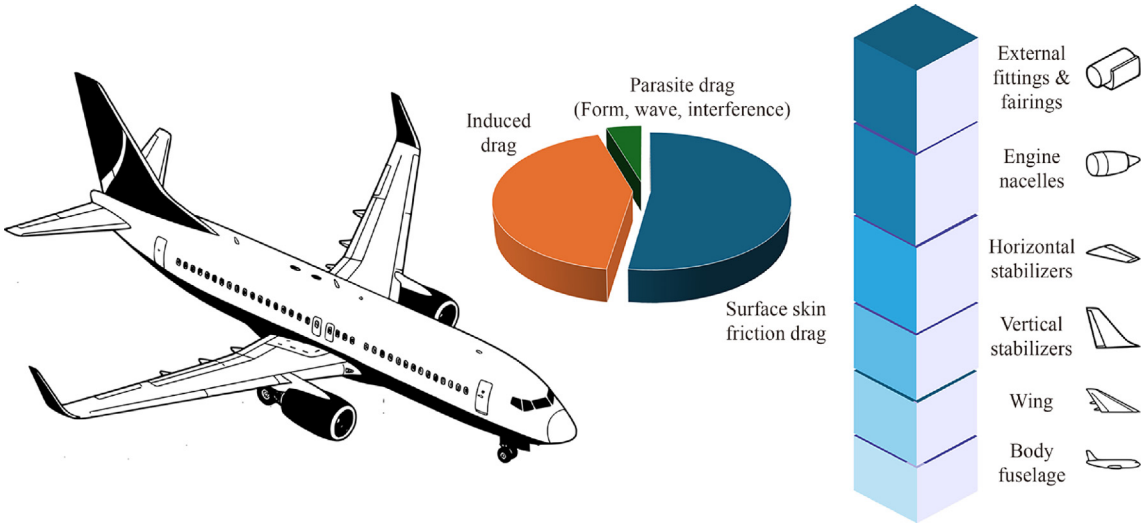


Fig. 1 Typical drag breakdown for a commercial airplane.

been demonstrated consistently in laboratory experiments,[2–5] numerical simulations,[6,7] and full-scale applications,[8] making them a canonical reference for near-wall flow manipulation (Table 1).

Despite the wide range of geometries and flow configurations investigated since their introduction, riblet performance exhibits a set of robust and unifying features. First, drag reduction is governed by viscous scaling and confined to the near-wall region, with little dependence on outer-layer parameters. Second, riblets operate within a narrow optimal window: measurable drag reduction occurs only when the riblet spacing is of the order of the viscous length scale, with a well-defined optimum around $s^+ \approx 15$ and a rapid transition to drag increase for larger sizes.[2,5,9,10] This behaviour, schematically illustrated in Fig. 2, establishes the classical distinction between a viscous drag-reducing regime and a roughness-dominated regime. The maximum drag reduction is generally associated with the groove geometry. The most widely investigated solutions are blade, v-shaped and parabolic profiles, with corresponding maximum values of drag reduction ranging between 8% and 10%. In the specific case of v-shaped (also typically referred to as triangular riblets), sensitivity to the tip angle has also been documented. This represents a significant challenge for the comparison between experiments and numerical simulations, owing to the technological limitations of reproducing exact and sharp tip angles.

The physical mechanism underlying riblet drag reduction is associated with a modification of near-wall turbulence. DNS studies have shown that riblets suppress spanwise velocity fluctuations[11] and weaken quasi-streamwise vortices in the buffer layer, leading to reduced Reynolds shear stress production.[6] From a modelling perspective, this behaviour can be interpreted in terms of an anisotropic wall response, whereby the surface presents low resistance to streamwise motion while significantly impeding spanwise flow.

The detailed groove geometry plays a central role in both the effectiveness and the breakdown of riblet performance. In the viscous regime ($s^+ \leq 10 - 15$), drag reduction increases approximately linearly with riblet size, but the achievable benefit depends on the groove cross-section. Sharper profiles tend to enhance near-wall anisotropy and yield higher peak drag reduction (see Fig. 2), whereas blunter profiles generally exhibit lower peak performance but improved robustness to manufacturing tolerances and surface degradation.[5] As riblet size increases toward and beyond the optimal regime, the influence of groove shape becomes more pronounced. DNS studies have shown that once turbulent motions penetrate into the grooves, drag reduction collapses rapidly and the surface behaviour transitions toward that of conventional roughness.[6,9,17] The dependence on the groove profile was embedded by García-Mayoral and Jiménez[7] into a single scaling parameter, which accounts not only for the spacing, but also for the cross-sectional area of the riblet geometry. In particular, $l_g^+ = \sqrt{A_g}$, where A_g is the cross-section of the groove. The optimal value of l_g^+ is of the order of 10–12.

Importantly, recent investigations have demonstrated that riblets can induce secondary motions and spanwise mean-flow inhomogeneities that enhance turbulent momentum transfer and increase drag, even for riblet sizes traditionally classified as being within or close to the viscous regime.[9,10,18] These findings highlight intrinsic limitations of canonical riblets and indicate that viscous scaling alone is not always sufficient to predict performance, particularly when geometry-induced secondary flows become significant.

Beyond fully resolved simulations, modelling approaches have been developed to assess riblet effects at application-relevant Reynolds numbers. Slip-length-based boundary conditions[19,20] and low-order predictive frameworks[21] have enabled the investigation of riblet performance on complex geometries and in the presence of pressure gradients, showing that riblets can influence not only skin friction but also displacement thickness and pressure drag.

2.1. Virtual origin and anisotropic wall response

Early theoretical interpretations of riblet drag reduction were based on viscous analyses of Stokes flow over grooved surfaces. Bechert and Bartenwerfer[4] introduced the concept of direction-dependent virtual origins, later formalised by Luchini et al.[22] and recently revisited Luchini and Chung[23] through the protrusion-height framework. In this model, drag reduction arises from the difference between effective streamwise and spanwise protrusion heights, $h_\parallel - h_\perp$, which represent the virtual displacements experienced by the flow, namely the drag reduction is $\sim \mu_0(h_\parallel - h_\perp)$.

This framework was unified and extended by García-Mayoral and Jiménez,[7] who interpreted riblets as a particular realisation of an anisotropic wall boundary condition. Within this perspective, drag reduction occurs when the streamwise virtual origin lies closer to the wall than the spanwise one, explaining both the existence of an optimal viscous-scaled riblet size and the confinement of drag reduction to a narrow parameter range.

More recent studies have refined this interpretation by highlighting the role of wall-normal transpiration at the riblet crests and its interaction with near-wall vortical structures.[24–27] These works suggest that the difference between the mean flow and the turbulence origin ($l_U - l_T$), rather than the mean-flow origin alone, provides a more consistent reference for comparing riblet and smooth-wall flows. Indeed, when the model introduced by Luchini et al.[22] is applied to riblet geometries with varying profiles, it exhibits considerable scatter in the proportionality coefficient μ_0. It must be noted that, while these refinements improve the physical interpretation of riblet effects, they do not alter the fundamental conclusion that

Table 1 Representative maximum turbulent skin-friction drag-reduction levels reported for common riblet groove profiles.

Groove profile	Max. drag reduction	Reference
Flow field	≈8%	Walsh[12]; Walsh and Lindemann[13]
Solid temperature field	10%	Bechert et al.[5]; Peet and Sagaut[14]
Species concentration field	≈9.8%	Sasamori et al.[15]; Cafiero and Iuso[16]

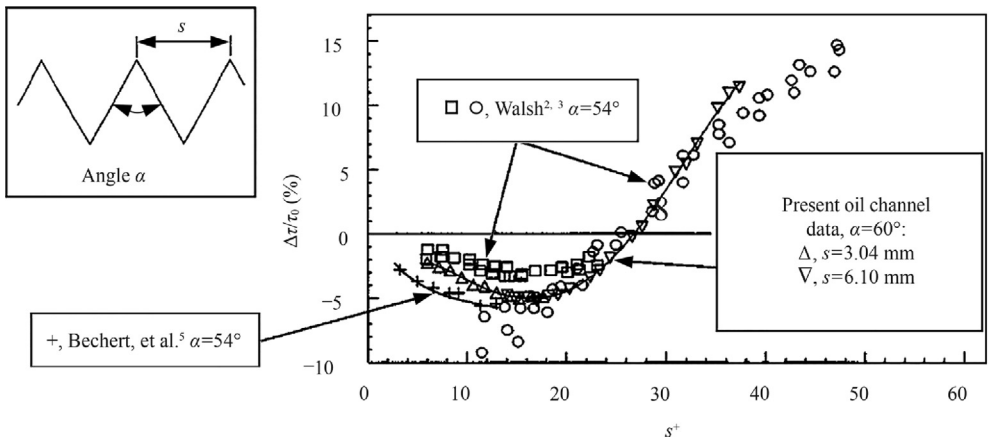


Fig. 2 Schematic representation of drag-reducing regimes observed on riblets (Reproduced with permission of CUP from Bechert et al.[5]).

canonical riblet drag reduction is a near-wall, viscous mechanism, which is fundamentally based on the concept of affecting the virtual origin of the flow. This model is schematically depicted in Fig. 3.[26]

Overall, canonical riblets provide a well-understood and repeatable mechanism for turbulent skin-friction reduction, but their effectiveness is inherently constrained by a narrow optimal parameter range, sensitivity to off-design conditions, and modest maximum drag reduction. These limitations form the primary motivation for exploring unconventional riblet geometries that seek to extend robustness, broaden the operational envelope, or introduce additional flow-control mechanisms beyond purely viscous near-wall anisotropy.

2.2. Off-design sensitivity: Yaw, pressure gradients, Reynolds number and compressibility effects

Riblet performance has been established primarily in canonical Zero-Pressure-Gradient (ZPG) turbulent boundary layers aligned with the mean flow, where optimal viscous-scaled spacings yield typical skin-friction reductions of the order of 5%–10%.[5,7,12] However, practical surfaces experience misalignment, non-equilibrium pressure gradients and very high Reynolds numbers, and the response of riblets to these off-design conditions is nuanced. Misalignment (yaw) systematically degrades performance because the riblet geometry ceases to suppress spanwise motion of near-wall vortices; experiments

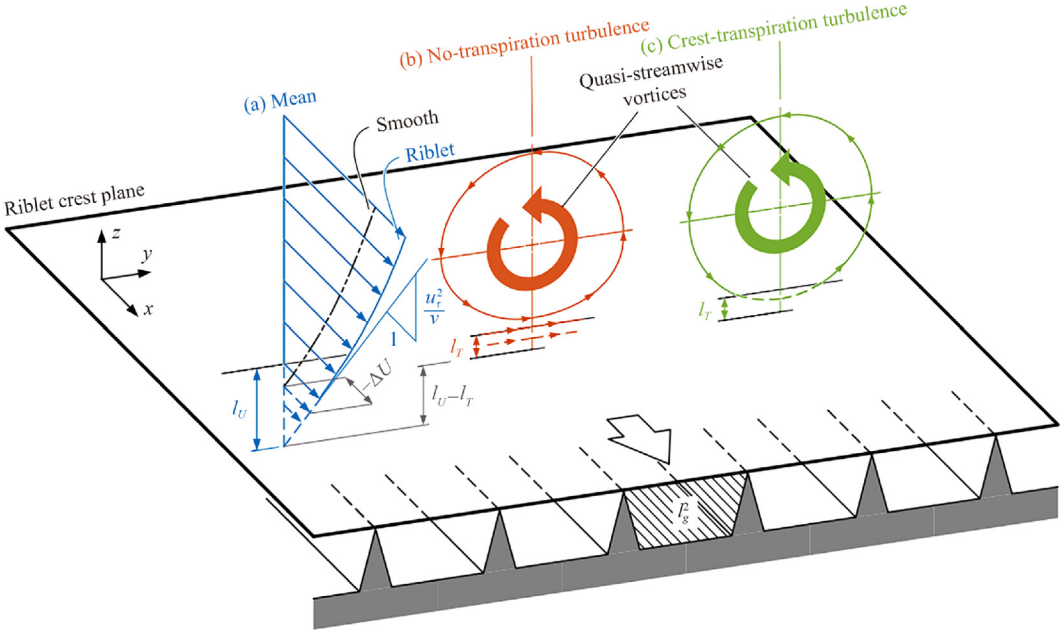


Fig. 3 Schematic representation of wall transpiration model proposed by Gómez-de-Segura et al,[24] Ibrahim et al[25] and Wong et al,[26] with indication of virtual origins of mean flow l_U of turbulence l_T, and their correspondence to drag reduction $-\Delta U = l_U - l_T$ (Image taken from Wong et al,[26] with permission from Cambridge University Press).

and DNS indicate a marked loss of benefit beyond modest yaw angles (typical critical values 10°–15°, depending on riblet immersion and shape) and near-vanishing gain at larger angles.[28]

Pressure-gradient effects are more subtle and, importantly, not universally detrimental: several wind-tunnel and numerical studies report only minor sensitivity of drag reduction to the pressure gradient commonly found on wings,[20] while Debisschop and Nieuwstadt[29] found that a moderate Adverse Pressure Gradient (APG) increased the measured drag-reduction percentage (e.g. from 7% to 13% in their tests). More recent LES/DNS and higher-Re experiments produce a mixed picture—mild APG may leave riblet performance essentially unchanged or slightly improved, whereas stronger APG can either reduce performance when outer-layer motions dominate the near-wall cycle (or when APG leads toward separation) or, conversely, enhance reduction in attached but strongly decelerating flows via APG-induced shear-layer/Kelvin–Helmholtz (KH) roller activity interacting with the riblet geometry Savino et al.[30] Therefore, the net effect of APGs depends on its strength, the absence of separated regions, riblet geometry and scaled size: when the inner-layer mechanism remains dominant and the flow stays attached, riblets frequently retain or even slightly improve their performance; when APG strengthens outer-layer forcing or leads to separation, the riblet benefit is reduced or lost. Finally, Reynolds-number scaling in viscous units (constant $s^+ = su_\tau/\nu$) remains a useful first-order predictor: most studies report little change in peak drag reduction up to moderately high Re_τ provided s^+ is maintained,[5,7] although subtle reductions and increased sensitivity to imperfections may appear at very large Re_τ where outer-layer modulation becomes significant.

Riblets have also been examined in compressible (transonic–supersonic) regimes,[31–33] motivated by the fact that a substantial fraction of drag in high-speed vehicles is still viscous and that riblets remain a purely passive, power-free technology whose near-wall mechanism (restriction of spanwise motion of the turbulence regeneration cycle) should persist as long as the grooves remain embedded in the viscous sublayer.[8,34] In transonic aerodynamics, wind-tunnel campaigns on airfoils have demonstrated that riblet films can deliver measurable profile-drag benefits on realistic configurations (e.g. supercritical sections at transonic conditions), supporting the broader conclusion of Viswanath's reviews that riblets can remain effective beyond low-speed flat-plate environments, although the net gain is highly sensitive to local pressure gradients, three-dimensionality, and surface-condition realism.[8] For supersonic/hypersonic turbulent boundary layers, high-fidelity simulations[35,36] show that skin-friction reduction can be obtained at high Mach numbers (including cold-wall conditions), but they also emphasize an aerothermal trade-off: the same geometric modifications that reduce τ_w can alter near-wall mixing and thus modify wall heat transfer in a non-trivial way, so that the "best" riblet design in high-speed flows may be constrained by thermal loads rather than drag alone. Beyond canonical ZPG high-speed boundary layers, recent high-speed studies targeting Shock-wave/turbulent-Boundary-Layer Interactions (SBLIs) indicate that riblet-like textures can influence separation/topology and unsteadiness in compression-ramp flows, which is promising but also highlights a key risk: texture–shock coupling may change separation behavior and loads, so performance must be assessed in the coupled aero–aeroelastic–thermal context rather than by extrapolating ZPG results.[37]

The main concerns about the adoption of riblets in transonic/supersonic regimes are both technological, owing to the necessity of maintaining the required viscous scaling across large variations in the values of the Reynolds number and local wall shear; also durability represents a factor, owing to contamination and thermal cycling; finally, the uncertain robustness in strongly non-equilibrium high-speed flows with shocks, separation, and three-dimensionality, the last of which is a known limiting factor also in incompressible flows.[8,35,37]

3. Unconventional riblets: Mechanisms and trade-offs

The limited drag-reduction margin and narrow optimal operating range of canonical, streamwise-aligned riblets have stimulated extensive research into non-canonical geometries. In these configurations, the grooves remain predominantly aligned with the mean flow, but their centreline, spacing, depth, or local orientation varies in the streamwise and/or spanwise directions. The objective is not merely geometric variation, but the introduction of additional physical mechanisms capable of complementing the classical riblet effect.

Conventional riblets primarily act through near-wall viscous anisotropy: by impeding spanwise motion, they modify the virtual origin perceived by the turbulent structures and weaken the near-wall cycle. In contrast, unconventional designs deliberately perturb the flow at larger scales. Depending on the geometry, they can impose controlled lateral forcing on quasi-streamwise vortices, generate spanwise pressure gradients, or induce organised secondary motions that redistribute momentum across the boundary layer. Their behaviour therefore extends beyond local viscous scaling arguments, and their effectiveness must be assessed through a global drag balance that includes not only skin-friction changes, but also pressure drag, dispersive stresses, and mean-flow reorganisation.

To enable a systematic comparison, the various designs are evaluated within a unified framework based on four recurring criteria: (A) the dominant physical mechanism introduced by the geometry; (B) robustness to off-design conditions, such as yaw, pressure gradients, and Reynolds-number variation; (C) the net drag balance between frictional benefits and non-friction penalties; and (D) scalability toward realistic configurations. This perspective highlights shared trade-offs and common failure modes that may remain obscured in isolated studies.

Within this framework, unconventional riblets can be broadly classified into three families.

The first comprises wave-like riblets, including sinusoidal and zigzag layouts, whose meandering centrelines introduce periodic spanwise forcing. Their primary mechanism is the controlled lateral displacement of near-wall vortical structures, with the intent of disrupting their coherence or weakening their lift-up action.

The second family includes spanwise-modulated geometries, such as converging–diverging riblets. By varying groove spacing or depth across the span, these designs create systematic spanwise pressure gradients that drive organised

secondary flows. These large-scale motions, often comparable in size to the boundary-layer thickness, redistribute momentum and alter the global shear profile.

The third family consists of hybrid or herringbone-like textures, which combine streamwise waviness with alternating orientation or spanwise modulation. These configurations represent the most pronounced departure from the canonical layout and intentionally couple lateral forcing with secondary-motion generation, leading to complex three-dimensional flow reorganisation.

In the following sections, each family is examined in detail, with emphasis on the governing mechanisms, performance limits, and the interplay between frictional gains and non-frictional penalties.

3.1. Wave-like riblets: Sinusoidal and zigzag grooves

A prominent route beyond canonical riblets is to impose a controlled, streamwise-periodic lateral waviness of the grooves. The earliest systematic studies of this idea were motivated by the analogy with active techniques such as spanwise wall oscillation[38,39]: by forcing the near-wall structures to follow a sinuous path, one aims to weaken quasi-streamwise vortices and reduce turbulent transport. Early numerical work explored sinusoidal riblets with triangular cross-sections and reported that drag reduction depends strongly on the wavelength and amplitude of the waviness, with the potential for improvements relative to straight riblets only in a limited range of parameters.[14,40]

By extending the Fukagata–Iwamoto–Kasagi (FIK) identity[41] to three-dimensional rough surfaces, the authors predicted that sinusoidal riblets could achieve greater drag reduction than straight, streamwise-aligned configurations. Their analysis indicated an overall increase in drag reduction, primarily associated with a decrease in the turbulent contribution to skin friction. These theoretical findings were corroborated by Large-Eddy Simulations (LES) conducted by the same group, which further showed that blade-type riblets yield the highest drag-reduction levels within this class of geometries.

More broadly, Peet and Sagaut[14] reported that, when the sinusoidal wavelength is appropriately tuned, wavy riblets can provide up to 50% additional skin-friction reduction compared with straight riblets. The improved performance was attributed to the transverse flow induced by the wall waviness, which generates a spanwise motion of near-wall structures analogous to that produced by spanwise wall oscillations.

Grüneberger et al.[42] investigated experimentally a turbulent channel flow manipulated with sinusoidal riblets, considering a range of amplitudes and wavelengths. The geometric forcing was characterized in wall units by the riblet deflection amplitude a^+ (approximately $5 < a^+ < 70$) and wavelength λ_x^+ (about $200 < \lambda^+ < 1400$), while the riblet geometry was defined by a trapezoidal cross-section with a fixed tip angle $\gamma = 30^\circ$. Their results did not show the same beneficial effects demonstrated by the large-eddy simulations of Peet and Sagaut,[14] possibly owing to the limited streamwise extent of the surface manipulation, which did not provide a sufficient distance for the onset of the drag reduction.

Mamori et al.[43] performed measurements on sinusoidal riblets with varying lateral spacing in a turbulent channel flow at friction Reynolds number 150, attaining values of drag reduction close to 12%, thus showing an improvement with respect to the typical straight riblets.

The geometric forcing was defined in wall units by a fixed streamwise wavelength $\lambda_x^+ = 360$ and by a spanwise riblet spacing s^+ varying sinusoidally in the streamwise direction between $s^+_{z,\min} = 15$ and $s^+_{z,\max} = 75$ with a riblet height $h^+ = 7.9$ and a riblet thickness $t^+ = 1.9$, as shown in Fig. 4.[43]

Subsequent investigations refined this picture and clarified that the net outcome of sinusoidal riblets is controlled by a balance between beneficial near-wall manipulation and detrimental penalties associated with added crossflow and pressure drag. Experiments in fully developed turbulent channel flow showed that sinusoidal riblets can yield appreciable drag reduction, with performance depending sensitively on waveform parameters and on the extent to which the geometry reduces the effective wetted area while maintaining near-wall anisotropy.[15,44]

The sinusoidal riblet configurations, with a geometry similar to that shown in Fig. 4, were characterized in wall units by a riblet height h^+ ranging from 3.75 to 8.5, a fixed average spanwise spacing $s^+ = 42.27$, a riblet thickness t^+ between 1.8 and 5.4, and a streamwise wavelength λ_x^+ varied from 107.9 to 431.6.

DNS-based parametric studies reached similar conclusions: Okabayashi[45] identified optimal combinations of amplitude and wavelength for which modified sinusoidal riblets outperform their straight counterparts, but also showed that off-design parameters can rapidly degrade performance by increasing pressure drag and by reorganising the near-wall motions in an unfavourable way.

In more recent boundary-layer experiments, Cafiero and Iuso,[16] Cafiero et al.[46–48] further demonstrated that sinusoidal riblets, with spanwise spacing s^+ ranging from 7 to 11, a streamwise wavelength λ_x^+ between 450 and 680, and a forcing amplitude a^+ varying from 3.5 to 5.3, can exert a strong influence on the organisation of low-speed streaks, and their effect can become more pronounced in the conditions where drag reduction is the largest. The analysis of the two-points correlations allowed the authors to claim a loss of coherence of the near-wall organised structures when the wavy riblets were deployed compared with canonical straight riblets. This was also confirmed by an overall attenuation of energy content of the near-wall structures characterized by a streamwise wavelength of about $\lambda^+ \approx 1000$, which is associated with the near-wall streaks. This confirmed the effect of the riblets in tamper-

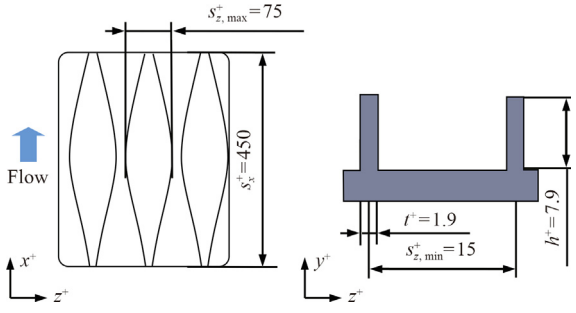


Fig. 4 Schematic representation of geometry of sinusoidal riblet used in Mamori et al.[43]

ing with the near-wall turbulence generation cycle, effectively manipulating the organization of the streaks.

Subsequent DNS simulations showed that the effect of the streamwise modulation of the groove is such that generates a modulation of the counter-rotating vortices originating at the riblets' crests. Fig. 5 shows the modulation of the quasi-streamwise aligned vortices generated near the tip of the grooves at different locations along the sinusoidal riblet. The results are obtained from DNS simulations of a turbulent channel flow at a friction Reynolds number of 540. The simulations were performed using an immersed boundary method as proposed by Jelly and Busse.[49] It is clear how, in correspondence of the maximum amplitudes of the wavy riblets, a single coherent structure is formed. This picture is aligned with the hypothesis formulated by Cafiero and Iuso,[16] in the case of a turbulent boundary layer manipulated by sinusoidal riblets. Following the argument of Wong et al.,[26] this must be somehow linked to the drag reduction mechanism, with a specific indication of the effect on the wall transpiration induced by such vortices.

Fig. 6 displays the effect of the surface geometry on the turbulence origin. The wavy geometries (left panels) show that the value of l_T^+ is dependent on the riblet geometry. In particular, while the longitudinal case displays a uniform distribution both in span and in the streamwise direction, the sinusoidal case is instead characterized by a wavy pattern. The peak-to-peak separation is equal to half the wavelength of the sinusoidal geometry, and the maximum value l_T^+ is found in correspondence with the maximum amplitudes of the sine wave (i.e. where there is a change in the concavity of the groove). The periodicity in the value of l_T^+ suggests that the sinusoidal geometry is indeed tampering with the near-wall turbulence and with a direct footprint on the drag reduction (see bottom row).

Zigzag riblets constitute a closely related class, often viewed as a piecewise-linear approximation of a sinusoidal waviness, and sometimes linked to Miura-fold patterns. In particular, all riblet configurations share a triangular streamwise cross-section with a tip angle of 90°, while the spanwise spacing and height are kept fixed at $s^+ = 18$ and $h^+ = 9$, respectively. The streamwise wavelength is set to $\lambda_x = 565$ whereas the yaw angle β is varied over the range 0° (straight riblet), 10.1°, 19.6°, 24.0°, and 28.1°. DNS investigations showed that zigzag riblets can reduce skin friction under appropriate geometric conditions, but with a strong dependence on the zigzag angle and wavelength Okabayashi et al.[50] Recent experiments have continued to explore how zigzag riblets modify the multi-scale organisation of turbulence in boundary layers, providing evidence that their effect extends beyond simple viscous scaling when the lateral modulation becomes sufficiently strong Fan et al.[51] Overall, the literature suggests that wave-like riblets can match or slightly exceed straight-riblet performance for carefully chosen parameters, but they generally introduce additional design sensitivities (wavelength selection, increased pressure drag, and robustness to flow direction), making their net benefit highly configuration-dependent.

3.2. Converging-diverging and spanwise varying riblets

A second major branch of unconventional designs introduces *spanwise heterogeneity* through Converging-Diverging (C-D) patterns, in which groove spacing, groove depth, or local orientation varies gradually in the spanwise direction. This concept is often inspired by biological textures and has also been proposed as a route to generate controlled spanwise motions that could modify the boundary layer more profoundly than canonical riblets. Early experimental work on C-D riblets focused on establishing the fundamental flow topology. Xu et al.[52] studied a laminar boundary layer over finite-length C-D riblets and showed that these textures generate a systematic spanwise flow from the diverging lines toward adjacent converging lines, accompanied by weak recirculating secondary motions. Although laminar, this result is important because it anticipates a recurring feature observed in turbulent investigations: spanwise-varying riblets tend to induce secondary flows whose scale is set by the C-D wavelength (often comparable to the boundary-layer thickness), rather than by the riblet spacing.

When extended to turbulent flows, this family of surfaces reveals a central trade-off: while local riblet-like regions may reduce skin friction, the globally induced secondary motions and associated pressure gradients can impose a non-negligible penalty, potentially offsetting (or even overwhelming) the

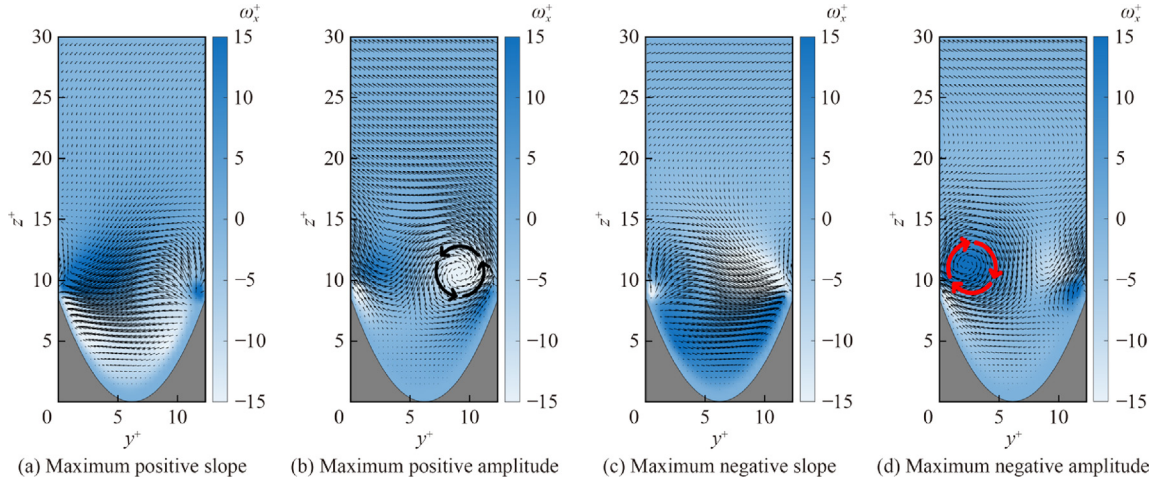


Fig. 5 Time-averaged velocity contour plots at different location along sine groove.

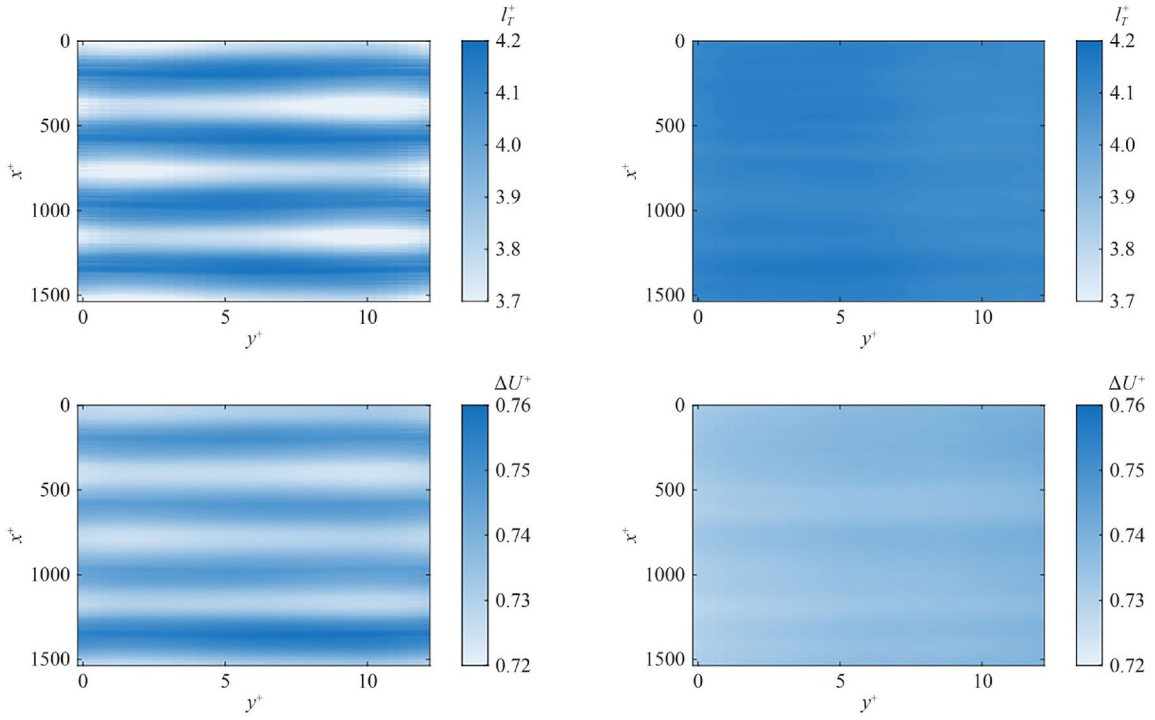


Fig. 6 Turbulence origin l_T^+ and drag reduction ΔU^+ calculated for sinusoidal (left panels) and longitudinal (right panels) riblets (Flow is from top to down).

friction benefit. DNS and high-fidelity simulations have repeatedly highlighted this competition for C-D and herringbone-like patterns.[53] A representative outcome is that certain C-D configurations can achieve local skin-friction reduction, but often at the expense of increased pressure drag or enhanced mean advection in the diverging regions, leading to modest net gains or even net drag increases depending on wavelength and geometry.[53] Recent turbulence-resolving computations have also examined transition and boundary-layer development over riblets with alternating converging and diverging patterns, indicating that the interplay between induced secondary flow, near-wall anisotropy, and the natural instability mechanisms of the boundary layer can be complex.[53]

Closely related are spanwise-varying riblets, as the one presented in the previous section43 designed explicitly to reorganise turbulence through large-scale heterogeneity. Recent DNS work has shown that sufficiently large and spanwise-modulated riblets can trigger strong dispersive stresses and robust secondary motions that reshape the mean flow and turbulence distribution across the layer.[18] While such reorganisations can be exploited to tailor the flow, they also tend to depart significantly from the classical riblet mechanism and can push the surface response toward roughness-like behaviour unless the modulation is carefully constrained. These findings reinforce a key message for a review: once riblet designs deliberately introduce spanwise heterogeneity, performance can no longer be interpreted solely through local viscous scaling or protrusion-height arguments, and the net drag outcome becomes a coupled problem involving secondary flows, dispersive transport, and pressure-drag contributions.

3.3. Zigzag/converging–diverging hybrids and herringbone-like arrangements

A third family combines wave-like centrelines and spanwise modulation into a herringbone layout, inspired for example by bird-feather textures. Although these surfaces are not strictly streamwise-parallel everywhere, they are often discussed alongside C-D riblets because they incorporate alternating converging/diverging zones and can be manufactured as a repeating pattern. DNS studies have provided an important cautionary result: herringbone textures can behave similarly to canonical riblets only when the spanwise wavelength of the pattern is very large, while at smaller wavelengths they tend to generate strong secondary flows that increase drag substantially.[54] In this study the authors explore different parameters for herringbone riblets. All cases share a blade-type riblet geometry with zero thickness, a fixed spanwise spacing $s^+ = 17$ and a height-to-spacing ratio $h/s = 0.5$, corresponding to a maximum riblet height $h^+ \approx 17$. The herringbone pattern is defined by the riblet inclination angle α, varied between 0°, 15°, and 165°, and by the number of grooves per feather half-width N_{groove} ranging from 1 to 128. This results in a wide range of spanwise texture wavelengths (feather widths), spanning from $\Lambda_f^+ \approx 35$ up to $\Lambda_f^+ \approx 4500$.

This mechanism mirrors the C-D trade-off discussed above and provides a clean numerical demonstration that inducing strong secondary motion is generally detrimental to net drag reduction in turbulent channels. More recent experimental work has begun exploring herringbone riblets in compressible

and shock-interaction contexts, broadening the application space but also introducing additional coupling between geometry-induced secondary flows and outer-layer dynamics.[37]

3.4. Summary of physical mechanisms

Although unconventional riblet geometries have been explored across a wide range of configurations, their reported performance remains highly scattered and often difficult to interpret within a unified framework. This dispersion reflects the fact that non-canonical riblets introduce additional physical mechanisms beyond those governing classical, streamwise-aligned riblets. In this section, the dominant mechanisms and failure modes are synthesized to provide a coherent interpretation of the existing literature.

Classical riblets achieve drag reduction by introducing a strongly anisotropic response in the near-wall region, selectively impeding spanwise motion while minimally affecting streamwise flow. This mechanism is intrinsically viscous and confined to the buffer layer, which explains both the robustness of straight riblets and the narrow window of effective viscous-scaled sizes.

Unconventional riblets attempt to enhance or supplement this mechanism by introducing geometric modulations that act beyond purely viscous effects. Wave-like riblets, for instance, impose a controlled lateral forcing that can weaken near-wall quasi-streamwise vortices, while spanwise-varying and converging–diverging patterns deliberately introduce spatial heterogeneity. However, once these modulations induce flow responses that scale with outer units rather than viscous units, the separation of scales underpinning the classical riblet mechanism is progressively lost. As a result, the flow response transitions from a near-wall modification to a global reorganisation of the boundary layer.

Across a broad class of unconventional designs, the emergence of persistent secondary motions represents the most consistent mechanism leading to performance degradation. While weak, localised secondary flows may coexist with friction reduction, large-scale secondary motions—typically spanning a significant fraction of the boundary-layer thickness—introduce enhanced wall-normal and spanwise transport, increased Reynolds stresses, and non-negligible pressure-drag contributions. Conventional, straight riblets also lead to an added share of drag, as pointed out by Modesti et al.[18] Dispersive stresses are indeed associated with the spanwise heterogeneity of the flow, which for drag-reducing riblets is typically confined to the roughness layer, whose depth is provided as a linear function of the riblets' spacing.[18] This added share of drag is, however, small compared to the friction contribution for optimal riblets.

Despite reducing the skin friction drag, unconventional riblets' arrangements can lead to further inhomogeneities in the flow. This behaviour is particularly evident for converging–diverging and herringbone-like riblets, where spanwise modulation generates mean crossflows whose characteristic length scale is decoupled from the riblet spacing. Once secondary motions become energetically significant, the surface response increasingly resembles that of three-dimensional roughness, even when local riblet dimensions remain within the nominal viscous regime. These observations suggest that secondary motions should be regarded not as a secondary effect, but as a primary failure mode for non-canonical riblet designs.

From a drag-budget perspective, the net benefit of unconventional riblets therefore depends on a delicate balance between friction reduction and non-friction penalties. Designs that introduce only mild modulation can preserve a favourable balance, whereas aggressive geometric variations tend to shift the surface response toward a roughness-dominated regime. This framework provides a unifying explanation for why unconventional riblets can outperform straight riblets in carefully tuned configurations, yet frequently fail to deliver robust net drag reduction under realistic conditions.

These trends are summarised in Table 2, which provides a conceptual comparison of the dominant mechanisms and limitations across different riblets designs.

4. Critical assessment framework: Robustness, scalability, net drag balance, and off-design sensitivity

A recurring limitation of the unconventional riblet literature is that performance is often discussed primarily in terms of local skin-friction variation, while the overall aerodynamic impact is controlled by the balance between friction reduction and additional penalties such as pressure drag, dispersive stresses, and mean-flow reorganisation.[18,20,54] This is particularly relevant for three-dimensional textures, where geometry-induced secondary motions can contribute substantially to the drag budget.[53,54] To enable a consistent comparison across design families four metrics are identified: (A) robustness (repeatability across parameter variations and tolerance to

Table 2 Conceptual comparison of canonical and unconventional riblet families, highlighting dominant physical mechanisms, potential benefits, and typical limitations.

Riblet family	Dominant mechanism	Potential benefit	Typical penalty	Robustness
Straight riblets	Near-wall viscous anisotropy	Moderate, repeatable drag reduction	Rapid break-down beyond optimal viscous-scaled size	High
Sinusoidal riblets	Controlled lateral forcing of near-wall structures	Comparable or slightly higher than straight riblets in tuned cases	Added pressure drag and strong parameter sensitivity	Medium
Zigzag riblets	Multi-scale modulation of streaks and vortices	Local drag reduction for selected angles and wavelengths	High sensitivity to geometry and flow direction	Low–Medium
Converging–diverging riblets	Induced secondary motions	Local skin-friction reduction in favourable regions	Global drag increase due to crossflow and pressure drag	Low
Herringbone-like textures	Large-scale flow reorganisation	Limited or none	Strong secondary motions and roughness-like behaviour	Very low

imperfections); (B) sensitivity to off-design conditions; (C) net drag balance (competition between skin-friction reduction and non-friction penalties); and (D) scalability toward realistic Reynolds numbers and application-relevant configurations.[8,19,20] The qualitative trends discussed below align with the mechanism-driven summary in Table 2, which should be interpreted as a map of dominant trade-offs rather than a universal performance ranking.

- For wave-like riblets, the literature broadly agrees that a controlled lateral forcing can modify near-wall structures and, in tuned cases, yield drag reduction comparable to or slightly exceeding straight-riblet performance.[14–16,40,43,44,47] DNS and experiments indicate that the outcome is governed by the forcing parameters (wavelength, amplitude, and local orientation) and by how these parameters interact with the near-wall cycle and quasi-streamwise vortices.[43,45,47] A unified scaling for the impact of the additional geometric parameters, such as the amplitude and the wavelength of the riblet profile has not been demonstrated yet.

  A key inconsistency concerns the magnitude and robustness of the reported gains: some numerical predictions suggest large improvements for selected parameter ranges,[40,45] whereas experiments have reported either modest gains or a stronger dependence on the extent of the manipulated patch and on geometric details.[16,42,44] This discrepancy plausibly reflects finite-length effects and configuration-specific penalties (e.g. crossflow/pressure-drag contributions) that are not always isolated or reported consistently across studies.[42,43]

  As a result, wave-like riblets if on one side may broaden the range of flow configurations at which they deliver drag reduction,[16] they may also require a longer streamwise distance for the onset of the effects (Table 2).

  For this family, reporting skin-friction reduction alone can be misleading because the lateral modulation can introduce additional losses through crossflow and pressure-drag contributions, especially for larger forcing amplitudes.[42,43] Evidence for scalability toward realistic Reynolds numbers and complex boundary-layer conditions is still limited, with most results obtained in channels or controlled boundary layers.[16,47] Overall, wave-like designs should be regarded as configuration-tuned devices rather than universal upgrades over canonical riblets.[14,45]
- Spanwise-varying and C-D riblets: studies consistently report that the geometry induces mean secondary motions and dispersive stresses whose characteristic scale is set by the modulation wavelength, often comparable to the boundary-layer thickness.[52,53] This mechanism represents a qualitative departure from the canonical near-wall anisotropy paradigm and explains why these designs are frequently associated with low robustness.[53] Apparent disagreements in the literature—ranging from local skin-friction reductions to net drag increases—can be rationalised by recognising that the global drag response is controlled by the competition between local viscous benefits and secondary-motion/pressure penalties.[18,53] However, a unified criterion predicting when the balance becomes favourable is still lacking, and outcomes remain sensitive to modulation wavelength, Reynolds number, and configuration (transition versus fully turbulent boundary layers). This makes cross-study comparisons difficult when drag is not decomposed into friction and non-friction components. From a drag-budget standpoint, this family is intrinsically high-risk: secondary motions enhance wall-normal and spanwise transport, typically increasing Reynolds stresses and introducing additional pressure-drag contributions. Off-design sensitivity is therefore expected to be strong, and extrapolation to realistic flows with pressure gradients and curvature remains uncertain. At present, the maturity of C-D riblets as robust net-drag reducers appears limited, despite their potential as flow-tailoring textures.
- Herringbone-like arrangements: DNS evidence shows that herringbone-like riblets generally generate strong secondary motions and mean-flow reorganisation, and that net drag reduction is only observed when the texture wavelength is very large; at smaller wavelengths, drag increases can be substantial.[54] This behaviour supports the interpretation of secondary motions as a primary failure mode for aggressive three-dimensional patterns and motivates the very low robustness classification in Table 2.

The outcomes depend strongly on wavelength and inclination, which limits the generalisability of isolated positive results. In addition, compressible/shock-interaction contexts introduce further coupling between secondary flows and outer-layer dynamics, and the net impact remains configuration-dependent. A key open point is therefore not whether secondary motions arise, but whether they can be constrained sufficiently—while preserving near-wall anisotropy—to yield a positive net drag balance under realistic conditions.[37,54]

From the summary, two clear messages emerge. First, unconventional riblets can plausibly outperform canonical riblets only when they preserve near-wall anisotropy while strictly limiting geometry-induced secondary motions; this condition is most plausibly met by mild wave-like modulations rather than by strongly spanwise-varying textures. Second, for unconventional riblets, reporting skin-friction reduction alone is insufficient: drag budgets separating friction, pressure drag, and dispersive/secondary-flow contributions are required to establish whether a configuration provides a genuine net benefit. As an example, the added share of pressure drag arising in the case of wavy riblets is quite limited, yet it is expected to be significantly larger for more aggressive geometric modifications. Similarly, the effects of dispersive stresses can lead to additional drag, which, especially in off-design conditions, may limit the benefits of unconventional designs.

5. Data-driven and AI-assisted design of riblets and passive wall textures

The design of riblets and, more broadly, passive wall textures for turbulent drag reduction is intrinsically a high-dimensional optimisation problem. Even for canonical riblets, performance is confined to a narrow viscous-scaled window and depends on geometric details (tip sharpness, groove opening, cross-sectional area), while unconventional and three-dimensional

textures introduce additional degrees of freedom that make exhaustive parametric studies quickly impractical. This has motivated growing interest in data-driven and Artificial-Intelligence (AI) methods as accelerators of (A) geometry exploration, (B) surrogate modelling of drag responses, and (C) robustness-oriented optimisation across operating conditions.

A clear example of AI-enabled optimisation applied directly to riblets is the work of Lee et al.,[55] who combined large-eddy simulation with mixed-variable Bayesian optimisation in a design-by-morphing framework to search a continuous space of riblet geometries in turbulent channel flow. Their methodology illustrates an emerging paradigm for passive surface design: high-fidelity simulations provide expensive but reliable evaluations, while Bayesian optimisation navigates the design space efficiently and returns candidate geometries that may depart from classical intuition.

Complementary to optimisation, data-driven modelling can provide fast predictors of drag changes for families of wall textures and roughness-like surfaces, which can then be embedded within optimisation loops. For instance, Lee et al.[56] proposed a transfer-learning framework to predict drag on irregular rough surfaces using limited DNS data, leveraging empirical correlations as inductive bias. Although not riblet-specific, this approach is directly relevant to unconventional riblets and textured surfaces, for which producing sufficiently large high-fidelity datasets remains a bottleneck.

From the perspective of physics and design objectives, the riblet problem can be framed as a special case of the broader roughness and texture literature, in which drag outcomes depend on the balance between viscous effects and form-drag/pressure-drag contributions. A comprehensive synthesis of this viewpoint and of modern predictive approaches for rough-wall drag is given by Chung et al.,[57] which highlights how geometric descriptors and surface statistics relate to drag and why generalisation across texture classes is challenging. For riblets and near-riblet textures, this reinforces the need to move from single-condition optimisation toward mapping of performance and robustness envelopes.

Importantly, AI-based methods are most valuable when they are embedded in a physics-informed, multi-objective formulation. For wall textures, optimising skin-friction reduction alone may lead to geometries that increase pressure drag or trigger secondary motions, especially for three-dimensional textures. Thus, the optimisation objective should ideally include drag-budget components (e.g. friction vs. pressure/dispersive contributions) and robustness constraints (e.g. sensitivity to Reynolds number, pressure gradients, yaw, and manufacturing deviations). In this sense, AI should be viewed as a tool to accelerate exploration and optimisation under physically meaningful constraints, rather than as a replacement for turbulence understanding. Broader perspectives on how machine learning supports modelling, optimisation, and control in fluid mechanics are reviewed by Brunton et al.,[58] and many of these principles (surrogate modelling, uncertainty awareness, and data efficiency) apply directly to passive wall-texture design.

Overall, the literature suggests that data-driven optimisation and modelling can substantially accelerate riblet and wall-texture design, particularly for unconventional geometries where the parameter space is large. However, success hinges on dataset quality, objective-function design (net drag rather than friction alone), and explicit accounting for robustness across operating conditions.

6. Conclusions

This review has examined unconventional riblet geometries through a mechanism-driven and drag-budget-oriented perspective, with the explicit aim of assessing whether and how non-canonical designs can overcome the intrinsic limitations of classical, streamwise-aligned riblets. The analysis leads to a clear overarching conclusion: while unconventional riblets can locally enhance or modify near-wall turbulence, their net aerodynamic benefit is fundamentally constrained by the balance between skin-friction reduction and geometry-induced penalties, most notably pressure drag and secondary-motion-driven losses.

Canonical riblets remain the most mature and robust passive drag-reduction concept. Their mechanism—near-wall viscous anisotropy—has been consistently validated across experiments, DNS, and full-scale applications, and their limitations are now well understood.[5,7,8,22,23,26] Unconventional riblets do not constitute a universal improvement over this baseline. Instead, they introduce additional physical mechanisms that can either complement or undermine the canonical riblet effect, depending on how strongly they disturb the near-wall and outer-layer flow.

Among unconventional designs, wave-like riblets (sinusoidal and zigzag) emerge as the most promising candidates for modest performance gains beyond straight riblets. When carefully tuned, they can preserve near-wall anisotropy while introducing a controlled lateral forcing that weakens near-wall coherent structures.[40,43,45,47] However, their benefits are highly parameter-dependent and sensitive to off-design conditions, finite-length effects, and crossflow-induced pressure penalties, which limits robustness and complicates extrapolation to realistic configurations.[42,44,50] As such, wave-like riblets should be regarded as configuration-specific devices rather than as broadly applicable upgrades.

In contrast, spanwise-varying, converging--diverging, and herringbone-like riblets consistently highlight the risks associated with aggressive three-dimensionality. Although local skin-friction reduction may occur in favourable regions, the dominant and recurring outcome is the generation of large-scale secondary motions whose characteristic scale is set by the modulation wavelength rather than by viscous units.[18,53,54] These secondary motions enhance wall-normal and spanwise transport, introduce dispersive stresses, and generate additional pressure drag, often overwhelming any viscous benefit. The resulting behaviour increasingly resembles that of three-dimensional roughness, explaining the low robustness and limited net-drag-reduction maturity of these concepts.

A key implication of this review is that reporting skin-friction reduction alone is insufficient for assessing unconventional riblets. For three-dimensional textures, the net aerodynamic outcome is controlled by the full drag budget, including pressure drag and secondary-flow contributions, which are not always isolated or reported in the literature.[18,54] Apparent contradictions among studies can often be

reconciled when results are interpreted through this drag-budget lens rather than through local friction metrics alone.

In the light of this review, several directions emerge for future research pathways:

- Drag-budget-resolved assessments: future studies should systematically decompose drag into skin-friction, pressure, and dispersive contributions, enabling unambiguous evaluation of net benefits for three-dimensional riblet textures. Without such decomposition, cross-study comparisons remain inherently limited. This also calls for a consistent exploitation of fully resolved numerical simulations and experiments, to complement the lack of scalability to large values of the Reynolds number of the former, and the often limited information of the latter.
- Robustness and off-design performance: the sensitivity of unconventional riblets to yaw, pressure gradients, curvature, surface contamination, and manufacturing tolerances must be explicitly quantified. Robustness envelopes, rather than single-point optimal results, are required to assess practical relevance.
- Scalability toward realistic configurations: evidence for performance at high Reynolds numbers and in application-relevant boundary layers remains sparse. Reduced-order models and wall-modelled LES approaches offer a promising route for exploring scalability beyond canonical flows through numerical simulations. On the other hand, experiments should focus on more realistic flow scenarios.
- Physics-informed design and optimisation: data-driven and machine-learning-based optimisation frameworks hold significant potential for exploring the high-dimensional design space of unconventional riblets. However, their effectiveness will depend on embedding physical constraints—such as limiting secondary-motion intensity and pressure-drag penalties—rather than optimising skin-friction reduction alone.[21]

In summary, unconventional riblets should not be viewed as a replacement for canonical designs, but as specialised, configuration-tuned surfaces whose success hinges on a delicate balance between near-wall anisotropy and outer-layer disruption. A shift toward drag-budget-aware analysis, robustness-focused evaluation, and physics-informed optimisation is essential if unconventional riblet concepts are to progress from isolated demonstrations toward reliable and scalable drag-reduction technologies.

CRediT authorship contribution statement

Enrico AMICO: Writing – review & editing, Methodology, Investigation, Data curation, Conceptualization. **Gioacchino CAFIERO:** Writing – review & editing, Writing – original draft, Supervision, Methodology, Funding acquisition, Conceptualization.

Declaration of competing interest

The authors declare that they have no known competing financial interests or personal relationships that could have appeared to influence the work reported in this paper.

Acknowledgements

The authors wish to acknowledge the financial support of the GREENER project – funded by the European Union – Next Generation EU within the PRIN 2022 program (D.D. 104 - 02/02/2022 Ministero dell'Università e della Ricerca).

References

1. Kornilov V. Combined blowing/suction flow control on low-speed airfoils. *Flow Turbul Combust* 2021;**106**(1):81–108.
2. Walsh MJ. Drag characteristics of V-groove and transverse curvature riblets. *Viscous flow drag reduction*. Reston: AIAA; 1980. p. 168–84.
3. Walsh MJ. Turbulent boundary layer drag reduction using riblets. *20th aerospace sciences meeting*. Reston: AIAA; 1982.
4. Bechert DW, Bartenwerfer M. The viscous flow on surfaces with longitudinal ribs. *J Fluid Mech* 1989;**206**:105–29.
5. Bechert DW, Bruse M, Hage W, et al. Experiments on drag-reducing surfaces and their optimization with an adjustable geometry. *J Fluid Mech* 1997;**338**:59–87.
6. Choi H, Moin P, Kim J. Direct numerical simulation of turbulent flow over riblets. *J Fluid Mech* 1993;**255**:503–39.
7. García-Mayoral R, Jiménez J. Drag reduction by riblets. *Philos Trans A Math Phys Eng Sci* 2011;**369**(1940):1412–27.
8. Viswanath PR. Aircraft viscous drag reduction using riblets. *Prog Aerosp Sci* 2002;**38**(6–7):571–600.
9. Gatti D, von Deyn L, Forooghi P, et al. Do riblets exhibit fully rough behaviour? *Exp Fluids* 2020;**61**(3):81.
10. von Deyn LH, Gatti D, Frohnapfel B. From drag-reducing riblets to drag-increasing ridges. *J Fluid Mech* 2022;**951**:A16.
11. Bottaro A. Flow over natural or engineered surfaces: an adjoint homogenization perspective. *J Fluid Mech* 2019;**877**:P1.
12. Walsh MJ. Riblets as a viscous drag reduction technique. *AIAA J* 1983;**21**(4):485–6.
13. Walsh MJ, Lindemann AM. Optimization and application of riblets for turbulent drag reduction. *22nd aerospace sciences meeting*. Reston: AIAA; 1984.
14. Peet Y, Sagaut P. Theoretical prediction of turbulent skin friction on geometrically complex surfaces. *Phys Fluids* 2009;**21**(10):105105.
15. Sasamori M, Iihama O, Mamori H, et al. Parametric study on a sinusoidal riblet for drag reduction by direct numerical simulation. *Flow Turbul Combust* 2017;**99**(1):47–69.
16. Cafiero G, Iuso G. Drag reduction in a turbulent boundary layer with sinusoidal riblets. *Exp Therm Fluid Sci* 2022;**139**:110723.
17. García-Mayoral R, Jiménez J. Hydrodynamic stability and breakdown of the viscous regime over riblets. *J Fluid Mech* 2011;**678**:317–47.
18. Modesti D, Endrikat S, Hutchins N, et al. Dispersive stresses in turbulent flow over riblets. *J Fluid Mech* 2021;**917**:A55.
19. Mele B, Tognaccini R. Slip length–based boundary condition for modeling drag reduction devices. *AIAA J* 2018;**56**(9):3478–90.
20. Mele B, Tognaccini R, Catalano P, et al. Effect of body shape on riblets performance. *Phys Rev Fluids* 2020;**5**(12):124609.
21. Ran W, Zare A, Jovanović MR. Model-based design of riblets for turbulent drag reduction. *J Fluid Mech* 2021;**906**:A7.
22. Luchini P, Manzo F, Pozzi A. Resistance of a grooved surface to parallel flow and cross-flow. *J Fluid Mech* 1991;**228**:87–109.
23. Luchini P, Chung D. Higher-order homogenised riblet boundary conditions. *J Fluid Mech* 2026;**1030**:A2.
24. Gómez-de-Segura G, García-Mayoral R. Turbulent drag reduction by anisotropic permeable substrates–analysis and direct numerical simulations. *J Fluid Mech* 2019;**875**:124–72.
25. Ibrahim JI, Gómez-de-Segura G, Chung D, et al. The smooth-wall-like behaviour of turbulence over drag-altering surfaces: a unifying virtual-origin framework. *J Fluid Mech* 2021;**915**:A56.

26. Wong J, Camobreco CJ, García-Mayoral R, et al. A viscous vortex model for predicting the drag reduction of riblet surfaces. *J Fluid Mech* 2024;**978**:A18.
27. Bottaro A, Innocenti G, Ahmed EN. A slip-transpiration-vortex model for riblets past the viscous regime. *Meccanica* 2025;**60**(8):2487–506.
28. Klumpp S, Guldner T, Meinke M, et al. Riblets in a turbulent adverse-pressure gradient boundary layer. *5th flow control conference*. Reston: AIAA; 2010.
29. Debisschop JR, Nieuwstadt FTM. Turbulent boundary layer in an adverse pressure gradient: Effectiveness of riblets. *AIAA J* 1996;**34**(5):932–7.
30. Savino BS, Rouhi A, Wu W. Attached decelerating turbulent boundary layers over riblets. *AIAA Scitech 2026 forum*. Reston: AIAA; 2026.
31. Catalano P, de Rosa D, Mele B, et al. Performance improvements of a regional aircraft by riblets and natural laminar flow. *J Aircr* 2020;**57**(1):29–40.
32. Mele B, Tognaccini R, Catalano P. Performance assessment of a transonic wing–body configuration with riblets installed. *J Aircr* 2015;**53**(1):129–40.
33. Kaneko K, Oyama A, Yakeno A. Viscous drag reduction effect of riblets in compressible flow. *J Aircr* 2026, Epub 2026 Mar 4.
34. Viswanath PR. Riblets on airfoils and wings: A review. *30th fluid dynamics conference*. Reston: AIAA; 1999.
35. Duan L, Choudhari M. Effects of riblets on skin friction and heat transfer in high-speed turbulent boundary layers. *50th AIAA aerospace sciences meeting including the new horizons forum and aerospace exposition*. Reston: AIAA; 2012.
36. Duan L, Choudhari MM. Direct numerical simulations of high-speed turbulent boundary layers over riblets. *52nd aerospace sciences meeting*. Reston: AIAA; 2014.
37. Wen B, Zhong S, Wang G, et al. Effects of herringbone riblets on shock-wave/turbulent boundary-layer interactions. *Aerosp Sci Technol* 2024;**146**:108914.
38. Quadrio M, Ricco P. Critical assessment of turbulent drag reduction through spanwise wall oscillations. *J Fluid Mech* 2004;**521**:251–71.
39. Ricco P, Skote M, Leschziner MA. A review of turbulent skin-friction drag reduction by near-wall transverse forcing. *Prog Aerosp Sci* 2021;**123**:100713.
40. Peet Y, Sagaut P, Charron Y. Turbulent drag reduction using sinusoidal riblets with triangular cross-section. *38th fluid dynamics conference and exhibit*. Reston: AIAA; 2008.
41. Fukagata K, Iwamoto K, Kasagi N. Contribution of Reynolds stress distribution to the skin friction in wall-bounded flows. *Phys Fluids* 2002;**14**(11):L73–6.
42. Grüneberger R, Kramer F, Wassen E. Influence of wave-like riblets on turbulent friction drag. In: Tropea C, Bleckmann H, editors. *Nature-inspired fluid mechanics: Results of the DFG priority programme 1207 "nature-inspired fluid mechanics" 2006–2012*. Berlin: Springer; 2012. p. 311–29.
43. Mamori H, Yamaguchi K, Sasamori M, et al. Dual-plane stereoscopic PIV measurement of vortical structure in turbulent channel flow on sinusoidal riblet surface. *Eur J Mech B* 2019;**74**:99–110.
44. Sasamori M, Mamori H, Iwamoto K, et al. Experimental study on drag-reduction effect due to sinusoidal riblets in turbulent channel flow. *Exp Fluids* 2014;**55**(10):1828.
45. Okabayashi K. Direct numerical simulation for modification of sinusoidal riblets. *J Fluid Sci Technol* 2016;**11**(3):JFST0015.
46. Cafiero G, Amico E, Serpieri J, et al. Effects of sinusoidal riblets on turbulent boundary layer flow structures. *Progress in turbulence X*. Cham: Springer Nature Switzerland; 2024. p. 263–8.
47. Cafiero G, Amico E, Iuso G. Manipulation of a turbulent boundary layer using sinusoidal riblets. *J Fluid Mech* 2024;**984**:A59.
48. Cafiero G, Amico E, Serpieri J, et al. Conditioning turbulent boundary layers with sinuosoidal riblets. *AIAA aviation forum and ascend 2024*. Reston: AIAA; 2024.
49. Jelly TO, Busse A. Reynolds and dispersive shear stress contributions above highly skewed roughness. *J Fluid Mech* 2018;**852**:710–24.
50. Okabayashi K, Hirai K, Takeuchi S, et al. Direct numerical simulation of turbulent flow above zigzag riblets. *AIP Adv* 2018;**8**(10):105227.
51. Fan ZY, Hou ZX, Chen GH, et al. Scale arrangements in the turbulent boundary layer flow over a zigzag riblet surface. *Phys Fluids* 2025;**37**(3):035114.
52. Xu F, Zhong S, Zhang SY. Vortical structures and development of laminar flow over convergent-divergent riblets. *Phys Fluids* 2018;**30**(5):051901.
53. Jain I, Sarkar S. Insights of flow transition over converging-diverging riblets using large-eddy simulation. *Phys Fluids* 2025;**37**(7):074125.
54. Benschop HOG, Breugem WP. Drag reduction by herringbone riblet texture in direct numerical simulations of turbulent channel flow. *J Turbul* 2017;**18**(8):717–59.
55. Lee S, Moazam Sheikh H, Lim DD, et al. Bayesian-optimized riblet surface design for turbulent drag reduction *via* design-by-morphing with large eddy simulation. *J Mech Des* 2024;**146**(8):081701.
56. Lee S, Yang JS, Forooghi P, et al. Predicting drag on rough surfaces by transfer learning of empirical correlations. *J Fluid Mech* 2022;**933**:A18.
57. Chung D, Hutchins N, Schultz MP, et al. Predicting the drag of rough surfaces. *Annu Rev Fluid Mech* 2021;**53**:439–71.
58. Brunton SL, Noack BR, Koumoutsakos P. Machine learning for fluid mechanics. *Annu Rev Fluid Mech* 2020;**52**:477–508.